JOURNAL OF MATERIALS SCIENCE 31 (1996) 835–841

Modelling the softening within the fracture process zone associated with the fissuring mode of crack growth in Zr–2.5Nb CANDU pressure tube material

E. SMITH
Manchester University-UMIST Materials Science Centre, Grosvenor Street, Manchester M1 7HS, UK

P. H. DAVIES
Materials and Mechanics Branch, Chalk River Laboratories, Chalk River, Ontario, Canada K0J 1J

The fissuring mode of fracture in CANDU pressure tube material, and in particular Stage 1 crack growth (essentially flat J_R curve) as observed in some irradiated compact toughness specimens has been investigated. Models are presented of the fracture process zone associated with a crack that tunnels at the specimen mid-section, which extends preliminary work reported earlier. Various types of process zone behaviour are analysed, and based on an appropriate value for J_c, the J value associated with the cumulative mode of crack propagation in irradiated material, together with an estimate of the tensile stress at the leading edge of the process zone, the known failure mechanism (formation, growth and coalescence of voids) of the ligaments between the fissures is shown to be reasonably consistent with the experimental measurements of the fissure spacing and fissure length.

1. Introduction

The presence of microsegregated species (chlorine and carbon as carbide), has been shown [1] to be a primary factor responsible for the observed variability in toughness of Zr–2.5Nb pressure tube material. Such species can lead to premature decohesion in the axial (extrusion) direction of the tube on the transverse–axial plane. Such decohesion is manifested by the presence of strips of low-energy fracture (SLEFs) on this plane and results in a fractographic feature called fissures being observed on the radial–axial plane [1]. Such fissures have been observed on radial–axial fractures of both unirradiated and irradiated pressure tube material [1, 2], and it has been demonstrated [1, 2] that the large variation in toughness of such material, as measured by deformation J-integral–crack growth resistance curves (J_R curves) from small curved compact specimens, is clearly related to the tendency for fissure formation. It has been argued [1, 2] that the fissures effectively divide the material into a series of thin ligaments, each of which can then fail by a ductile mechanism at a reduced fracture strain. In the absence of fissure formation, it has been shown [1, 2] that very high toughness (J_R curve) may be achieved.

Because fissures have been shown to have an important effect on the fracture behaviour, it is highly desirable to quantify, by micro-mechanical modelling, how they affect the shape of the J_R curve. An earlier paper [3] described how the fissuring mode of fracture can be considered within Cottrell's categorization [4] of fracture modes into two types: cumulative and non-cumulative. A preliminary attempt was also made to model the fracture process zone associated with the fissuring flat fracture mode of crack growth in irradiated pressure tube material. This paper extends this earlier work. Based on an appropriate value for J_c, the J value associated with the cumulative mode of crack propagation in irradiated material, coupled with an estimate of the tensile stress at the leading edge of the process zone, the perceived failure mechanism (formation, growth and coalescence of voids) of the ligaments between the fissures is shown to be reasonably consistent with the experimental measurements of the fissure spacing and the fissure length.

2. Previous work on modelling the effect of fissures

Previously it was recognized [1, 2] that the failure of material displaying fissures consisted of two stages: (a) the formation of SLEFs lying in planes containing the axial and transverse direction, manifesting themselves as fissures lying in the axial direction in the plane of macroscopic crack growth, and (b) the failure of the ligaments between these SLEFs. Such a mechanism was supported by fractographic studies [1, 2] of the mid-section of curved compact specimens, which demonstrated an increase in fissure density (decreasing fissure spacing and increasing fissure length) with decreasing toughness (J_R curve) in both irradiated and unirradiated material; lower toughness (more highly

0022–2461

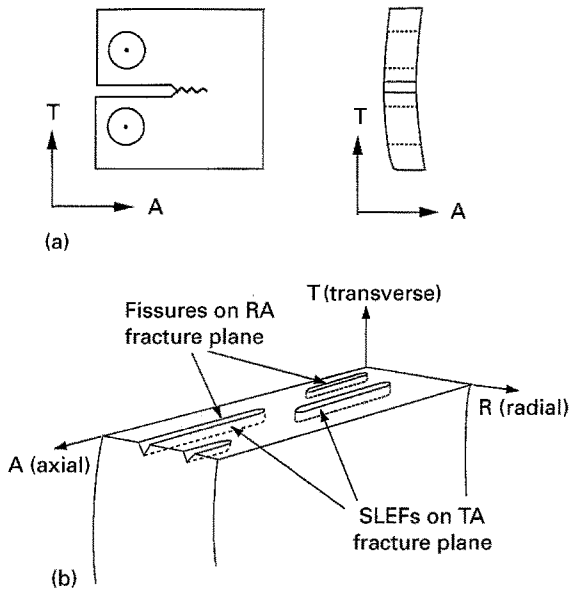

Figure 1 The relation between the specimen geometry, fracture plane and crack propagation direction to the pressure tube geometry.

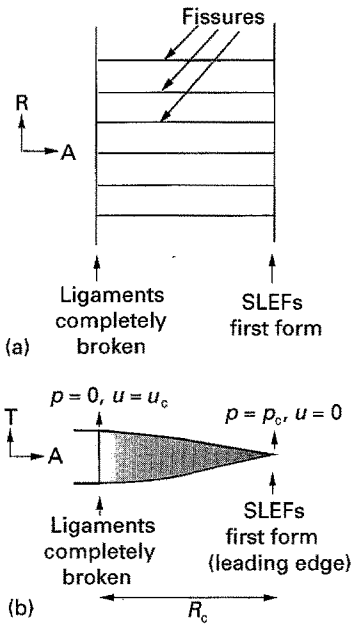

Figure 2 View of the cumulative mode fracture process zone: (a) looking down on fracture surface, and (b) side view. R is the radial or through-wall direction, T is the transverse or loading direction, and A is the axial or crack growth direction. The figure shows the positions where SLEFs first form, i.e. where the material first fractures, and where the ligaments are completely broken and there is then a complete loss of cohesion.

fissured) material having a "woody" appearance. With irradiation it was noted [2] that the density of fissures increased and the woody appearance of the fractures was enhanced; deep transverse–axial cracks were also occasionally present along the base of the fissures. The ligaments generally failed by ductile fibrous fracture (formation, growth and coalescence of voids); however, the dimple size was generally smaller, and there was also an increased tendency for shear between closely spaced fissures, with the irradiated material.

It was from this basis that the authors showed [3] how the fissuring mode of fracture could be considered within Cottrell's categorization [4] of "cumulative" and "non-cumulative" fracture modes. It was suggested [3] that when fissuring is pronounced, fracture can then proceed in a "cumulative" manner, requiring little further expenditure of energy once initiated. For example, narrow ligaments in irradiated material may easily fail by shear or sliding-off due to the low work hardening and strain localization behaviour. On the other hand, additional necking and/or void nucleation is required before the failure of wider ligaments. If the whole thickness of a cross-section were able to fail via a cumulative mode, then fracture would be unstable and proceed at a constant J value, with a zero crack tip opening angle, CTOA. In fact, instabilities (discrete increments of unstable crack growth) have been noted during small specimen testing of irradiated material [2], the failure of material in a cumulative manner (at a constant J value and a zero CTOA) being best displayed near the onset of crack extension with material that exhibits pronounced fissuring. This is manifested by a flattening of the J_R curve, termed Stage 1 crack growth, and is associated with a tendency for crack front tunnelling at the more highly constrained specimen mid-section.

Fig. 1 relates the specimen geometry, fracture plane and crack propagation direction to the pressure tube geometry, where the transverse direction refers to the circumferential or hoop direction of the tube. In modelling the fracture process zone associated with a crack propagating via the cumulative mode, the behaviour of a process zone associated with a semi-infinite crack in a remotely loaded infinite solid was considered [3]. This is a reasonable assumption, provided that the process zone is small compared with the test specimen's characteristic dimension (this aspect is referred to later). The process zone, which is of length R_c, extends from the position where the SLEFs first form (i.e. where the material first fractures) to the position where the ligaments between the SLEFs are completely broken and there is then a complete loss of cohesion (Fig. 2). In modelling the zone, the behaviour of the ligaments within the zone is averaged in such a way that the stress is p_c at the leading edge of the process zone where the SLEFs first nucleate and grow, and where the relative displacement, u, of the material within the zone is zero, while the stress, p, is zero at the trailing edge of the process zone where the ligaments are completely broken, and where the relative displacement, u, is equal to a critical value, u_c. The relation between p and u throughout the process zone depends on the way in which the ligaments between the SLEFs or fissures actually fail, and in the previous work [3] it was assumed that the relation between p and u was linear (Fig. 3).

For a semi-infinite crack in a remotely loaded infinite solid, and assuming a general p–u law, it may be shown using Rice's J-integral methodology [5] that the value of the J integral associated with crack propagation, i.e. J_c is

$$J_c = \int_0^{u_c} p(u)\,du \qquad (1)$$

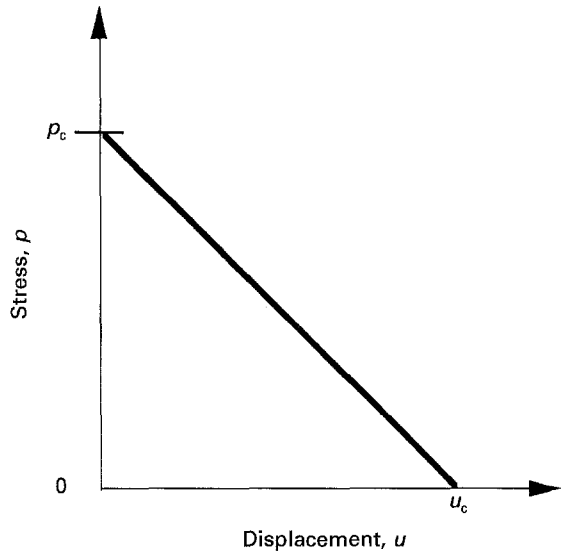

Figure 3 The linear relation between the stress, p, and the displacement, u, within the fracture process zone.

In the earlier work [3] the authors used the results of a previous analysis [6] for the size, R_c, of the process zone, which showed that for a general p–u law, though R_c is very dependent on the maximum stress p_c and the maximum displacement u_c, it is not overly dependent on the details of the p–u law, provided that the area under the p–u curve is $\gtrsim 0.2\, p_c u_c$. The authors argued that the relation [7] appropriate to the case where p retains a constant value p_c within the process zone, was a good enough working estimate for R_c, i.e.

$$R_c = \frac{\pi E_0 u_c}{8 p_c} \tag{2}$$

where $E_0 = E/(1 - \nu^2)$, E being Young's modulus and ν being Poisson's ratio. If the area under the p–u curve is $m p_c u_c$, where m is a constant whose value is less than unity ($m = 0.5$ for the linear variation in Fig. 3), then J_c is given by Equation 1 as

$$J_c = m p_c u_c \tag{3}$$

whereupon elimination of u_c between Equations 2 and 3 gives the equation

$$R_c = \frac{\pi E_0 J_c}{8 m p_c^2} \tag{4}$$

An appropriate value for J_c, the J value associated with the cumulative mode of crack propagation (Stage 1 crack growth in irradiated material showing pronounced fissuring), is $\sim 15\ \mathrm{kJ\,m^{-2}}$ [2]. Regarding the selection of a value for p_c, the tensile stress within the process zone at the leading edge where the SLEFs first form, the tensile yield stress of the material was used before [3], though accepting that the p_c value might be less; if p_c were to be greater than the tensile yield stress, then, following Cottrell's arguments [4], crack propagation would not be able to proceed via a cumulative mode. Thus with $p_c = 850$ MPa, a typical value for the transverse tensile yield stress of irradiated material at 240 °C [2], $J_c = 15\ \mathrm{kJ\,m^{-2}}$, $E_0 = 95 \times 10^3$ MPa and $m = 0.5$ (the linear p–u variation shown in Fig. 3), Equation 4 gives R_c as ~ 1.5 mm, a value which the authors believed [3] to be not unreasonable. This R_c value is markedly less than the initial crack depth or initial ligament width of the test specimen (~ 8.5 mm), and consequently use of the results from the analysis of a semi-infinite crack in a remotely loaded infinite solid is vindicated. With the same input values, Equation 3 gives u_c as ~ 35 μm. Because a typical mean fissure spacing, s_*, is ~ 60 μm for irradiated material [2] showing pronounced fissuring, then $u_c/s_* \sim 0.6$, which the authors viewed [3] to be not an unreasonable value when a thin ligament fails by a ductile fracture mechanism.

The next section presents a more comprehensive quantification of the process zone behaviour, making use of recent considerations of the behaviour of materials that can be modelled by a cohesive zone, which displays softening characteristics. Such materials are conveniently referred to as being elastic softening and include concrete, rock, reinforced ceramics and toughened polymers.

3. Detailed modelling of the process zone behaviour

Fig. 2b schematically shows how the displacement varies on moving away from the leading edge of the process zone, which is at the tip of a semi-infinite crack in a remotely loaded infinite solid. The governing relationship between the stress, p, and the displacement, u, is [8]

$$\frac{\mathrm{d}u}{\mathrm{d}s} = \frac{4 s^{1/2}}{\pi E_0} \int_0^{R_c} \frac{p(u)\,\mathrm{d}t}{(s - t) t^{1/2}} \tag{5}$$

with s being measured from the leading edge (see Fig. 2) and t being an integration variable. For the stress p to have a finite value p_c at the leading edge of the process zone, the total stress intensity at this position must be zero. This means that the stress intensity due to the applied loadings must equate with the stress intensity provided by the restraining stresses within the process zone. Because this stress intensity must equate with $K_{IC} = (E_0 J_c)^{1/2}$, it follows that

$$K_{IC} = (E_0 J_c)^{1/2} = \frac{2^{1/2}}{\pi^{1/2}} \int_0^{R_c} \frac{p(u)\,\mathrm{d}s}{s^{1/2}} \tag{6}$$

whereupon inversion of the integral Equation 5 coupled with the use of Equation 6 leads to Equation 1.

If we prescribe a relationship between the stress p and distance s as measured along the process zone, with $p = p_c$ at the leading edge and $p = 0$ at the trailing edge of the fully developed zone, Equation 5 gives a relation between the displacement u and distance s. This relation when coupled with the prescribed p–s relation, automatically leads to a p–u process zone law for which J_c can be determined via Equations 1 or 6, and for which R_c can be determined,

by recognizing that $u = u_c$ at the trailing edge of the process zone.

Without providing the complete details of the analysis which are presented in a paper [9] on the behaviour of a cracked elastic softening solid subjected to tensile loading, this report considers a stress–distance relation within the process zone that is of the form

$$\frac{p}{p_c} = \left(1 - \frac{s}{R_c}\right)^{n+1/2} = (1 - w)^{n+1/2} \quad (7)$$

with n (not necessarily an integer) $> -1/2$, and $w = s/R_c$. With this relation, the stress p is equal to p_c at the leading edge of the process zone ($w = 0$) and is zero at the trailing edge of the zone ($w = 1$), which is assumed to be fully developed, i.e. $u = u_c$ at the trailing edge. Substitution in Equation 5 then gives

$$\frac{du}{dw} = \frac{4p_c R_c}{\pi E_0} w^{1/2} J_n(1 - w) \quad (8)$$

with $J_n(w)$ being given by the integral relation

$$J_n(w) = \int_0^1 \frac{\mu^{n+1/2}\, d\mu}{(\mu - w)(1 - \mu)^{1/2}} \quad (9)$$

where μ is an integration variable. Equations 8 and 9, when coupled with the condition $u/u_c = 1$ when $w = 1$, lead to the result

$$\frac{p_c R_c}{E_0 u_c} = 2^{2n-1} \frac{[\Gamma(n + 2)]^2 (2n + 3)}{[\Gamma(2n + 3)](2n + 2)} \quad (10)$$

while Equations 6 and 7 give the result

$$\frac{J_c}{p_c u_c} = \frac{\pi[\Gamma(2n + 3)](2n + 3)}{2^{2n+4}[\Gamma(2n + 2)]^2 (2n + 2)} \quad (11)$$

For cases where n is zero or is a positive integer, the relation between the displacement u and distance w assumes a simple form. Then Equation 9 gives $J_n(w)$ as

$$J_n(w) = \pi w^n \sum_{r=0}^{n} \frac{(2r)!}{(r!)^2 (4w)^r} \quad (12)$$

and then Equations 8, 10 and 12 give

$$\frac{1}{u_c}\frac{du}{dw} = \frac{2^{2n+1}[(n + 1)!]^2 (2n + 3)}{[(2n + 2)!](2n + 2)} \times w^{1/2}(1 - w)^n \sum_{r=0}^{n} \frac{(2r)!}{(r!)^2 [4(1 - w)]^r} \quad (13)$$

This equation can be integrated to give the u–w relation, noting that $u = 0$ when $w = 0$. For the particular cases $n = 0, 1, 2$, the results are, respectively

$$\frac{u}{u_c} = w^{3/2} \qquad (n = 0) \quad (14)$$

$$\frac{u}{u_c} = \frac{w^{3/2}}{3}(5 - 2w) \qquad (n = 1) \quad (15)$$

$$\frac{u}{u_c} = \frac{w^{1/2}}{15}(35 - 28w + 8w^2) \qquad (n = 2) \quad (16)$$

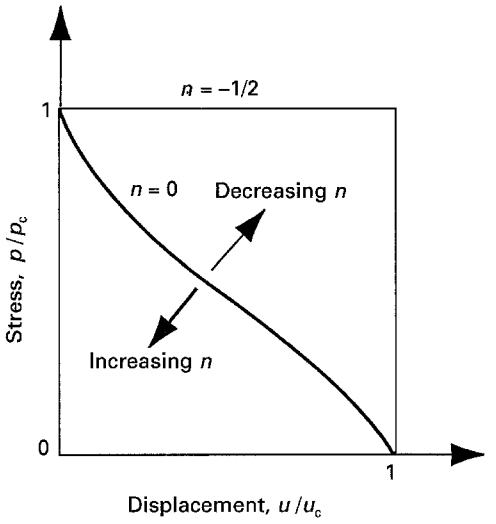

Figure 4 The range of power variation process zone laws analysed in Section 3.

These relations, when coupled with Equation 7, and by elimination of the parameter w, give a closed-form p–u process zone law for each particular value of n (zero or a positive integer); with $n = 0, 1, 2$ Equations 10 and 11 then give R_C and K_{IC} for each process zone law. As an example, for the simple case where $n = 0$, Equations 14 and 7 give the p–u law

$$\frac{p}{p_c} = \left[1 - \left(\frac{u}{u_c}\right)^{2/3}\right]^{1/2} \quad (17)$$

which was studied by Cribb and Tomkins [10]; this law approximates to a linear p–u law. The limiting case $n \to -1/2$ corresponds to the case where the stress in the process zone retains a constant value p_c, until the displacement u attains a critical value u_c when the stress falls abruptly to zero. For this special Dugdale–Bilby–Cottrell–Swinden (DBCS) process zone law [7, 11], Equations 10 and 11, respectively, give

$$\frac{p_c R_c}{E_0 u_c} = \frac{\pi}{8} \quad (18)$$

and

$$\frac{J_c}{p_c u_c} = 1 \quad (19)$$

these being standard results for the DBCS law. Fig. 4 shows (schematically) how the p–u softening law depends on the parameter n.

Equations 10 and 11, respectively, give the fracture process zone size R_c and J_c, the value of the J integral associated with crack propagation, and results are shown in rows 1 and 2 in Table I for $n = -1/2$ and for integer values of n from 0–5; the results in rows 1 and 2 are then used to give R_c in terms of p_c, E_0 and J_c and these results are given in row 3. With the input values used in the preceding section, i.e. $p_c = 850$ MPa, $E_0 = 95 \times 10^3$ MPa and $J_c = 15$ kJ m^{-2}, the results in Table I can be used to give u_c and R_c for various n values and the results are shown in Table II. It

TABLE I R_c and J_c for various process zone laws, i.e. n values

	n						
	$-1/2$	0	1	2	3	4	5
$\frac{R_c p_c}{E_0 u_c}$	0.393	0.375	0.417	0.467	0.514	0.559	0.600
$\frac{J_c}{p_c u_c}$	1.000	0.588	0.367	0.285	0.241	0.212	0.191
$\frac{R_c p_c^2}{E_0 J_c}$	0.393	0.638	1.136	1.868	2.133	2.637	3.141

TABLE II u_c and R_c for various process zone laws, i.e. n values. These results have been obtained using the input values $p_c = 850$ MPa, $E_0 = 95 \times 10^3$ MPa and $J_c = 15\,\mathrm{kJ\,m^{-2}}$

	n						
	$-1/2$	0	1	2	3	4	5
$\frac{J_c}{p_c u_c}$	1.000	0.588	0.367	0.285	0.241	0.212	0.191
u_c (μm)	18	30	48	62	73	83	92
R_c (mm)	0.77	1.26	2.23	3.68	4.20	5.19	6.19

should be noted that the preceding section's preliminary considerations used the same input p_c, E_0 and J_c values, but were based on a linear softening law, which (see Fig. 4) is close to the case for $n = 0$. In Section 3 it was shown that $u_c = 35$ μm and $R_c = 1.5$ mm, values that are similar to those of $u_c = 30$ μm and $R_c = 1.26$ mm obtained for the case of $n = 0$ (see Table II).

Now for irradiated material exhibiting pronounced fissuring, a typical mean fissure spacing, s_*, is ~ 60 μm [2]. That being the case, if n is low, say in the range $-1/2$–0, u_c ranges between 18 and 30 μm (see Table II), and u_c/s_* ranges between 0.3 and 0.5 which is a reasonable range of values when a thin ligament fails by the observed ductile fracture mechanism, i.e. formation, growth and coalescence of voids. It is also seen from Fig. 4 that when n lies within the range $-1/2$–0, the "softening" within the process zone is gradual, a behaviour which is consistent with the observed failure mechanism. Furthermore, the results in Table II show that with $-1/2 < n < 0$, R_c lies between 0.77 mm and 1.26 mm. The value for R_c is in the same range as the fissure length obtained for irradiated material which is highly fissured [2] (mean fissure length ~ 0.6 mm, maximum fissure length ~ 1.5 mm). This suggests that the fracture process zone R_c may be equated with the fissure length.

Thus, based on the experimental J_c value and an estimate of the tensile stress, p_c, at the leading edge of the process zone, there is reasonable consistency between the observed failure mechanism of the ligaments between fissures (the majority of which are expected to be associated with a gradual process zone softening behaviour), and the experimental measurements of the fissure spacing and fissure length. It is also clear that if the process zone softening behaviour is too pronounced, i.e. it is associated with a high n value > 0 (see Fig. 4), then the predicted value of u_c becomes unreasonably large, and the predicted value of R_c also becomes markedly greater than the range of experimentally measured fissure lengths. This conclusion, regarding inconsistency if there is pronounced softening in the process zone, is underpinned by the next section's results for a simple piece-wise process zone behaviour.

4. Piece-wise process zone behaviour

Fig. 5 shows a general and simple piece-wise process zone stress, p, versus displacement, u, law, where by varying the magnitudes of the parameters q and λ, a wide range of process zone behaviours can be modelled. The case where the parameters q and λ are both small, simulates a situation where the softening is very pronounced, i.e. there is an initially steep decline in the stress followed by a long tail. Adopting procedures similar to those for the power-law variation discussed in the preceding section, it can be shown [12] that the process zone size, R_c, and J_c, the value of the J integral associated with crack propagation, are given respectively by the expressions

$$\frac{p_c R_c}{E_0 u_c} = \frac{\pi}{8\,[q + 2\lambda + 2(\lambda^2 + \lambda q)^{1/2}]}$$

$$= \frac{\pi}{8\lambda[m + 2 + 2(1 + m)^{1/2}]} \tag{20}$$

$$\frac{J_c}{p_c u_c} = (q + \lambda)$$

$$= \lambda(m + 1) \tag{21}$$

with $q = m\lambda$. With regard to this section's objectives, we need only consider the case where $q = \lambda$ and

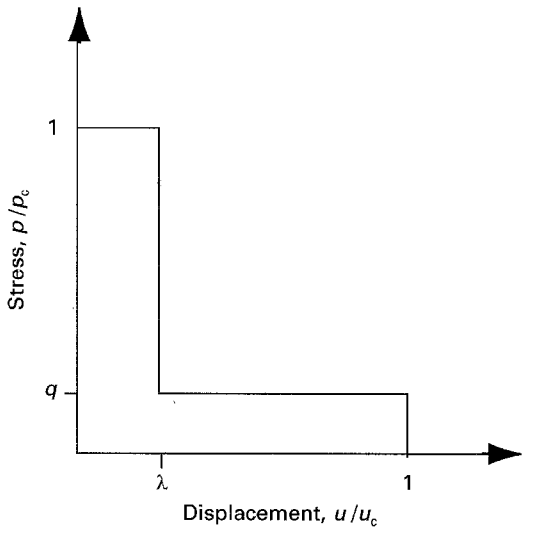

Figure 5 The piece-wise process zone stress–displacement law.

$m = 1$, whereupon Equations 20 and 21 simplify to

$$\frac{p_c R_c}{E_0 u_c} = \frac{\pi}{8\lambda(3 + 2(2)^{1/2})} \tag{22}$$

$$\frac{J_c}{p_c u_c} = 2\lambda \tag{23}$$

with elimination of u_c between these relations giving the relation

$$\frac{p_c^2 R_c}{E_0 J_c} = \frac{\pi}{16\lambda^2(3 + 2(2)^{1/2})} \tag{24}$$

With input values $p_c = 850$ MPa, $E_0 = 95 \times 10^3$ MPa and $J_c = 15\,\mathrm{kJ\,m^{-2}}$ and with a value of 0.1 for λ, Equations 23 and 24 show that u_c is equal to 88 μm and R_c is equal to 6.6 mm. This value of u_c is unreasonably large, because with the mean fissure spacing, s_*, being ~ 60 μm [2], then u_c/s_* is equal to 1.47 which is a high value even for ductile failure of the ligaments between the fissures. Moreover, the R_c value of 6.6 mm is an order of magnitude greater than the range of fissure lengths (mean fissure length ~ 0.6 mm, maximum fissure length ~ 1.5 mm) obtained experimentally [2] for highly fissured material. Thus we conclude that pronounced softening in the process zone is inconsistent with the experimental observations.

5. Discussion

The current work has been concerned with extending a model developed in an earlier paper [3] on the fissuring flat fracture mode of crack growth in irradiated Zr–2.5Nb pressure tube material. The starting point has been the recognition [1, 2] that failure of material displaying fissures can be broken down into two stages: (a) the formation of strips of low energy fracture (SLEFs) lying in planes containing the axial and transverse directions, and manifesting themselves as fissures on radial–axial fractures, and (b) the ductile failure of the ligaments between the SLEFs. In the earlier work [3] it was argued that Stage 1 (essentially zero J_R curve slope) crack growth in irradiated material proceeds by an essentially cumulative mode, using Cottrell's terminology [4], whereby non-linearity of material behaviour is confined to a thin region (the fracture process zone R_c) ahead of the crack tip. It was assumed that the average stress ahead of the crack equals the critical stress p_c when the SLEFs/fissures first nucleate and grow, and that final ligament failure occurs when the crack opening displacement resulting from this stress attains the critical displacement for ligament failure u_c. The present paper follows up this earlier work by providing a more detailed model of the fracture process zone associated with a crack that propagates via the fissuring mode.

Based on the experimentally measured J value J_c associated with the cumulative mode, and an estimate of the tensile stress, p_c, at the leading edge of the process zone, the known failure mechanism (formation, growth and coalescence of voids) of the ligaments between the fissures has been shown to be consistent with the experimental measurements of the fissure spacing and fissure length. In particular, for an elastic softening material associated with an n value in the range $-1/2$–0, the estimated fracture process zone size R_c (0.77–1.26 mm) was similar to the range of values obtained for the distribution of fissure lengths (mean fissure length ~ 0.6 mm, maximum fissure length ~ 1.5 mm). This is consistent with the statistical nature of the fracture process, because in practice there is actually a distribution of fissures and ligaments produced during crack growth, with narrower ligaments between longer (high R_c), more closely spaced fissures exhibiting more softening (lower n value) than wider ligaments between shorter (low R_c), more widely spaced fissures.

Notwithstanding this consistency, it is important to recognize that there are several issues which still merit further consideration; some of these were indicated in the earlier paper [3] and still remain unresolved. These key issues are given below.

1. It has been assumed that the tensile stress, p_c, within the process zone at its leading edge, where the SLEFs presumably first form, is the material's tensile yield stress. In practice, p_c could be less than the yield stress but it is unlikely to be greater than the yield stress following Cottrell's requirement [4] for crack growth to proceed via the cumulative mode.

2. Related to issue 1 is the criterion for SLEF formation since this might influence the value for p_c. If plastic deformation is important with regard to SLEF formation, then how is it influenced by irradiation hardening? Can the role of plastic deformation explain why SLEF formation and fissuring is more pronounced with irradiated material?

3. This paper has concentrated on the behaviour of irradiated material. We have to find an explanation as to why unirradiated material, though exhibiting a tunnelling behaviour, generally does not exhibit a pronounced Stage 1 flat J_R curve; presumably it is because a cumulative mode is unable to operate in the same way as it does with irradiated material. Is this because fissuring is less pronounced, or is it because ligament rupture with unirradiated material cannot proceed without there being some element of non-cumulative extension? What is the role of flow localization with regard to this issue?

4. The statistical nature of the fracture process also needs to be considered. Presumably there is a distribution of void nucleation conditions for SLEF/fissure formation depending upon the location of the microsegregated species with respect to the crack tip, as indicated by the distribution of fissures and ligaments produced during crack growth. This raises the question as to the existence of a critical density of fissures (fissure spacings and lengths) combined with a critical range of ligament fracture strains responsible for the cumulative fracture mode.

5. Finally, because the fractographic features (SLEFs and fissures) are merely a manifestation of the local crack tip stress state acting in the particular specimen geometry, how will the critical conditions producing such features be influenced by changes in specimen geometry (different crack tip constraints)?

This aspect of the fissuring flat fracture mode is particularly important with respect to applying results obtained from small curved compact (deeply cracked bend-type) specimens to the actual geometry of interest, i.e. a through-wall defect in a thin-walled tube under biaxial tension and bulging.

These issues have to be addressed before we have a complete picture of the fracture process zone associated with the cumulative mode of crack propagation in Zr–2.5Nb pressure tube material.

6. Conclusion

This paper has modelled in detail the fracture process zone associated with the fissuring flat fracture mode of crack growth in compact toughness specimens of irradiated Zr–2.5Nb pressure tube material. Based on an appropriate value for J_c, the J value associated with the cumulative mode of crack propagation in irradiated material, and an estimate of the tensile stress at the leading edge of the process zone, the observed failure mechanism (formation, growth and coalescence of voids) of the ligaments between the fissures has been shown to be consistent with the experimental measurements of the fissure spacing and fissure length.

Acknowledgement

The research described in this paper has been funded by the CANDU Owners Group, which the authors thank for permission to publish this paper.

References

1. I. AITCHISON and P. H. DAVIES, *J. Nucl. Mater.* **203** (1993) 206.
2. P. H. DAVIES, R. R. HOSBONS, M. GRIFFITHS and C. K. CHOW, in "10th International Symposium on Zirconium in the Nuclear Industry", ASTM STP 1245 (American Society for Testing and Materials, Philadelphia, PA 1994) p. 135.
3. E. SMITH and P. H. DAVIES, *J. Mater. Sci.* **30** (1995) 561.
4. A. H. COTTRELL, in "Proceedings of the First Tewksbury Symposium", University of Melbourne, Australia, edited by C. J. Osborn (Melbourne, 1965) p. 1.
5. J. R. RICE, in "Fracture", Vol. 2, edited by H. Liebowitz (Academic Press, London, 1968) p. 191.
6. E. SMITH, *Int. J. Eng. Sci.* **27** (1989) 301.
7. B. A. BILBY, A. H. COTTRELL and K. H. SWINDEN, *Proc. R. Soc.* **A272** (1963) 304.
8. J. R. WILLIS, *J. Mech. Phys. Solids* **15** (1967) 151.
9. E. SMITH, *Mech. Mater.* **17** (1994) 363.
10. J. L. CRIBB and B. TOMKINS, *J. Mech. Phys. Solids* **15** (1967) 135.
11. D. S. DUGDALE, *ibid.* **8** (1960) 100.
12. E. SMITH, *Mech. Mater.* **17** (1994) 369.

Received 14 August
and accepted 8 September 1995